EPSC Abstracts
Vol. 8, EPSC2013-667-1, 2013
European Planetary Science Congress 2013

Present day seasonal gully changes in a South Polar Pit on Mars.

J. Raack (1), D. Reiss (1), M. Vincendon (2), T. Appéré (3), O. Ruesch (1), and H. Hiesinger (1)
(1) Institut für Planetologie, Westfälische Wilhelms-Universität, Münster, Germany, (2) Institut d'Astrophysique Spatiale, Université Paris Sud, 91400 Orsay, France, (3) Laboratoire AIM, CEA-Saclay, DSM/IRFU/SAp, 91191 Gif-sur-Yvette, France (jan.raack@uni-muenster.de)

1. Introduction

Seasonal changes of gullies in the south polar region were first reported by [1,2]. These changes were observed within the Martian years (MY) 29 and 30 on slopes of polar pits. The polar pits are located in Sisyphi Cavi at -72.5°S and 355°E and have a depth of up to ~1000 m.

With high-resolution imaging, temperature and spectral data as well as spectral modeling, we analyze the exact timing of changes to detect the possible medium (CO_2, H_2O, or dry) and the mechanism which initiate present day gully activity. In our investigations we focus only on gullies in polar pits.

2. Background

Seasonal activity of gullies under current climatic conditions on Mars was observed by [1-6]. These observations were made on mountain and/or crater slopes [2-4], on dune slopes at mid-latitudes [2,5,6] and on slopes of polar pits [1,2]. The suggested mechanisms to form new gully deposits are melting of H_2O ice [3,5] or sublimation/removal of CO_2 ice [2,4,6].

Recent polar gullies in the southern polar region were also analyzed by [7]. On the basis of observations made with Mars Orbiter Camera (MOC) and Thermal Emission Spectrometer (TES), gully formation was proposed to result from sublimation of CO_2 ice in spring, triggering debris avalanches [7].

3. Data

Our investigations are based on multiple datasets, including Context Camera (CTX) images with a resolution of ~5 m/pxl and High Resolution Imaging Science Experiment (HiRISE) images with 0.25-1 m/pxl resolution from MY 29 to 31. All images of the study region were acquired in spring and summer. For detailed topographic information a HiRISE digital terrain model (HiRISE-DTM) was used (http://hirise.lpl.arizona.edu/dtm/dtm.php?ID=ESP_013097_1115).

Maximum surface temperature data of the study region were derived by TES (~3 km/pxl) between ~13:00 and ~15:00 local time. With near infrared spectral data based on the Compact Reconnaissance Imaging Spectrometer for Mars (CRISM) (18 and 36 m/pxl) and on the Observatoire pour la Minéralogie, l'Eau, les Glaces et l'Activité (OMEGA) spectrometer (1.5-4.8 km/pxl) we measured the strength of the CO_2 ice absorption band (1.43 µm) and H_2O ice absorption band (1.5 µm), respectively. These band strengths are complex non linear functions of amount of volatiles, grain size/texture, and mixture type [8].

4. Results

4.1 Image Analysis

Detailed analyses were made in a polar pit located in a filled crater (diameter ~54 km) north of Sisyphi Cavi at ~68.5°S and ~1.5°E. Modifications can be found within one gully at 1.44°E and -68.5°S.

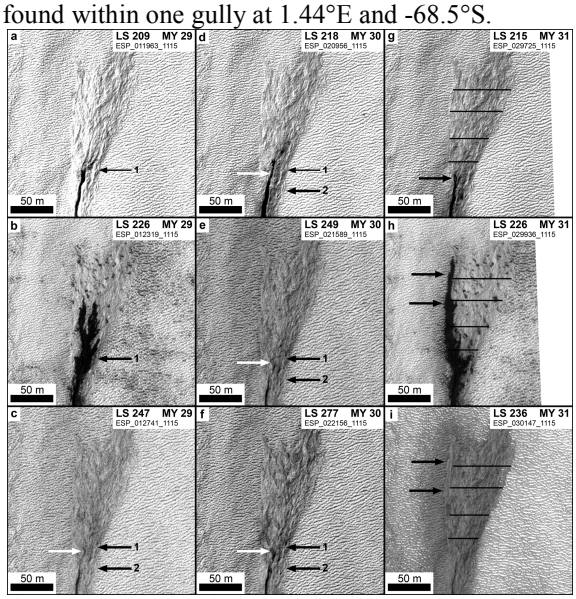

Figure 1: Sequence of seasonal behaviour of the gully with morphologic changes (apron and channel terminus) in spring of MY 29-31.

In Figure 1 the terminus of the gully channel and the apron are presented. The flow direction is from north to south. Dark material within the channel (Fig. 1a) leads to the formation of new dark deposits (Fig. 1b) between L_S 209° and 226° (beginning of spring) in MY 29 flowing ~70 m over the apron. The end of the gully channel is marked with a black arrow #1. At L_S 247° once ice has essentially disappeared (Fig. 2) deposition of material on the apron and within the channel shortens the channel by about 40 m (Fig. 1c; black arrow #2). The white arrow marks new

deposition on the gully apron (small knob). One year later in MY 30 at L_S 218° dark material can be found within the channel, flowing ~30 m over the apron (Fig. 1d). At the end of spring (L_S 249°) the dark material faded (Fig. 1e). Retreat of the channel is not detectable. At the end of spring (Fig. 1f) no more modifications were detected. In MY 31 at L_S 215° dark flow upon the apron is marked with a black arrow (Fig. 1g). The black horizontal lines represent the width of the gully apron. At L_S 226° a large dark flow at the western side of the gully apron is visible (Fig. 1h). This is comparable to the dark flow presented in Fig. 1b which occurs at the same time two Martian years before. At mid-spring (L_S 236°) a new deposit at the western side of the gully is visible (black arrows; Fig. 1i). New material was deposited in the area where the dark flow occurs. The black horizontal lines show a widening of the apron of about ~7 m.

4.2 Temperature and spectral analysis

TES data of the area analyzed in detail (area/line from 342°E to 7°E at -68.5°S) indicate that surface temperatures in autumn and winter are ~150 K. In mid spring (L_S ~220°) temperatures increase rapidly due to solar insolation and ice sublimation (Fig. 2). TES data show maximum surface temperatures up to ~285 K in early summer between L_S ~270° and ~310°.

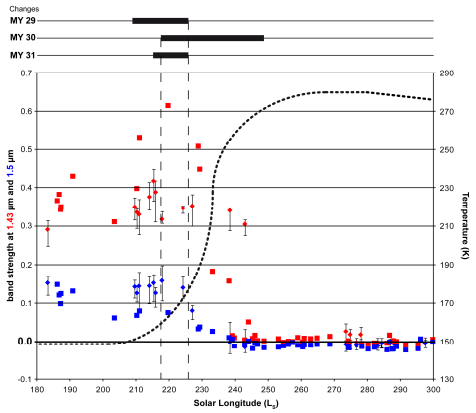

Figure 2: Measured maximum surface temperature (black dots) compared to values of CO_2 (1.43 µm) with CRISM (red diamonds) and OMEGA (red squares) and values of H_2O (1.5 µm) with CRISM (blue diamonds) and OMEGA (blue squares). First three lines represent the time range of gully changes (MY 29, 30, and 31).

For spectral analysis we processed data from CRISM (MY 28, and 29) and OMEGA (MY 27, 28, and 29). To better understand the temporal evolution of H_2O and CO_2, the band strengths of these volatiles (ices) in all available datasets at -68.5°S in the whole study region between L_s 180° to 300° were analyzed (Fig. 2). Detailed analyses show lowered ice band strengths within the gully with the dark flow. Although there are numerous gullies at the slope of the polar pit, only this single gully shows lowered band strengths.

5. Discussion and Conclusion

New small deposits on the gully apron, retreat of the gully channel due to infilling, and transport of dark material within the gully channel imply seasonal (volatile) activity. The activity of the large dark flow of the gully presented here can be constrained to occur between L_S 218° (Fig. 1d) and 226° (Fig. 1b,h). Spectral investigations show that CO_2 and H_2O ices sublimate rapidly between L_S ~220° and ~240° (Fig. 2). This is also the time range when temperatures rise rapidly and when gully changes occurred. Detailed analyses show that ice spectral signatures are generally lower on the dark flow features. This implies either 1) a generally lower value of volatiles within gully channels due to non uniform volatile deposition on the slope, 2) a faster sublimation of volatiles within gully channels, or 3) deposition of debris (dust/sand) above ice from the upslope regions by mass wasting.

1) The slope angle of the polar pit is very homogenous and numerous gully channels with comparable shapes and sizes can be found there (Fig. 1a). The only gully channel with lowered ice band strength is the gully with the dark flow. A non uniform deposition of volatiles in only one gully channel seems implausible. 2) If the volatiles sublimate faster within gully channels we would also expect lowered ice band strengths in other gully channels on the polar pit slope, which is not the case. 3) Deposition of material by mass wasting seems to be the most plausible scenario.

Here the dark flow deposits material (dust/sand) which covers a translucent slab of CO_2 ice with minor components of H_2O and dust. Spectral measurements show that the CO_2 ice signature within the dark flows is lower than its value in the surroundings but is not completely extinguished. This means that the interior of the gully consists in a subpixel mixing (>18 m/pxl) of covered and exposed icy surfaces. From spectral modeling of this subpixel mixing we estimate areal percentages of ~30% dust/sand + ~70% slab ice within the dark flows at L_S 216 in MY 28, assuming no dust/sand covers slab ice on the surroundings of the dark flows.

References

[1] Raack, J. et al. (2012) *LPS XXXIII*, Abstract #1801. [2] Dundas et al. (2012) *Icarus, 220,* 124-143. [3] Malin, M.C. et al. (2006) *Science, 314,* 1573-1577. [4] Dundas, C.M. et al. (2010) *GRL, 37*, doi:10.1029/2009GL041351. [5] Reiss, D. et al. (2010) *GRL, 37,* doi:10.1029/2009GL042192. [6] Diniega, S. et al. (2010) *Geology, 38,* 1047-1050. [7] Hoffman, N. (2002) *Astrobiology, 2,* 313-323. [8] Langevin et al. (2007) *JGR, 112,* E08S12.